Table 1. Observed fluctuations over a 100-km path on 19 June 1984. Symbols: f_c, carrier frequency; ν, rms phase rate.

f_c (Hz)	ν (mHz)
25	0.4
65	0.8
105	1.2
125	1.1
165	1.4
200	2.4

with range R in meters. To scale to the MIZ, we take the accepted model (*2*) and adjust Eq. 5 by the ratios of stability profile scale depth ($\approx 5.2 \times 10^{-2}$), surface stability frequency (≈ 2.3), acoustic axis stability frequency (≈ 12), inertial frequency (≈ 2.0), and sound speed change induced by vertical internal wave displacement (≈ 0.2), each of which appear in the model in various algebraic combinations. In choosing these ratios we are guided by internal wave measurements previously made in the same location and season in the MIZ (*12, 13*). The result (scaled to the MIZ) is

$$\nu \approx 2 \times 10^{-9} R^{1/2} f_c \qquad (6)$$

which for $R = 100$ km becomes $\nu \approx 6 \times 10^{-7} f_c$. This prediction falls more than one order of magnitude below our measurement (Eq. 3), and thus internal wave motion is not a plausible explanation for acoustic fluctuations in our measurements, although it is remotely possible given the uncertainties inherent in scaling from nonconcurrent internal wave data.

Phase rate fluctuations can be caused in a quiescent ocean by source-receiver motion through differential Doppler shift among the various acoustic paths, since each can be related to a differential angle with respect to the horizontal. Such differential Doppler fluctuations are observed in many experiments with drifting sensors (*10*) and, when large enough, can cause fluctuations that overwhelm those caused by ocean dynamics. We can estimate this phase rate as (*14*)

$$\nu' = a\, k_c\, \dot{R}\, (\Delta c/c)/2\pi \qquad (7)$$

where a is a constant dependent on the shape of the sound speed profile (estimated to be 0.5 for the Arctic), k_c is the carrier wave number, and $\Delta c/c$ is the incremental sound speed relative to the total sound speed defining the channel carrying the acoustic waves. For the MIZ we estimate $\Delta c/c$ to be about 10^{-2} and, from the observed range rate (≤ 0.3 msec^{-1}), find that ν' is less than approximately $10^{-6} f_c$. This is at least one order of magnitude less than our result; thus differential Doppler shift is also an unlikely mechanism for acoustic fluctuation.

If not internal waves or differential Doppler shift, and not drift accelerations or noise, then what is the cause? We have no answers, only hypotheses about possible ocean dynamical mechanisms. In addition to internal waves, the MIZ has dynamical structure associated with eddies, fronts, currents, and meanders (*1, 15*); we hypothesize that one or more of these can contribute to or dominate the phase rate. A crude model for fluctuations caused thereby is

$$\nu \approx \mu\theta^{-1} k_c R^{1/2} L^{1/2} \qquad (8)$$

where μ is the rms spatial contrast in index of refraction associated with the dynamical the corresponding structure, θ is characteristic time, and L the characteristic radius. Equation 8 is obtained from the phase fluctuations for Fresnel forward scattering (*16*), with θ as the most energetic period in the interval of observation. For the MIZ we estimate a value for μ of 4.9×10^{-3}, and with the observed value for ν we find that any other dynamical mechanism must have

$$2L/\theta^2 \approx 44 \text{ km day}^{-2} \qquad (9)$$

to fit the crude model.

If a mesoscale feature oscillates with the inertial period $\theta_i \approx 0.5$ day, then its scale $2L$ from Eq. 9 is 11 km, which is about that observed for underice eddies in the region of the acoustic experiment (*1*). Our observation period (0.42 day) is too short, and our model too crude, to conclude with confidence that eddy oscillations at the inertial period are indeed the most significant contributors. Instead we hypothesize that eddies or other mesoscale motions of comparable scale are important in determining acoustic fluctuations in the MIZ.

REFERENCES AND NOTES

1. T. O. Manley *et al.*, *Science* **236**, 432 (1987).
2. F. Dyson, W. Munk, B. Zetler, *J. Acoust. Soc. Am.* **59**, 1121 (1976).
3. W. R. Hamblen, thesis, Massachusetts Institute of Technology, Cambridge (1977).
4. P. N. Mikhalevsky, *J. Acoust. Soc. Am.* **72**, 151 (1982).
5. P. H. Dahl *et al.*, *ibid.* **79**, S69 (1986).
6. D. Sirmans and B. Bumgarner, *J. Appl. Meteorol.* **14**, 991 (1975).
7. D. S. Zrnic, *IEEE Trans. Aero. Elect.* **13**, 344 (1977).
8. ———, *ibid.* **15**, 613 (1979).
9. S. M. Flatte, Ed., *Sound Transmission Through a Fluctuating Ocean* (Cambridge Univ. Press, Cambridge, England, 1979).
10. R. P. Porter and R. C. Spindel, *J. Acoust. Soc. Am.* **61**, 943 (1977).
11. P. N. Mikhalevsky, *ibid.* **66**, 757 (1979).
12. M. D. Levine, C. A. Paulson, J. H. Morison, *J. Phys. Oceanogr.* **15**, 800 (1985).
13. O. M. Johannessen, J. A. Johannessen, S. Sandven, K. L. Davidson, in B. G. Hurdle, Ed., *The Nordic Seas* (Springer-Verlag, New York, 1986).
14. I. Dyer, paper presented at the Naval Research Laboratory Symposium on Underwater Acoustics, Washington, DC, February 1978.
15. O. M. Johannessen, J. A. Johannessen, E. Svendsen, R. A. Shuchman, W. J. Campbell, E. Josberger, *Science* **236**, 427 (1987).
16. L. A. Chernov, *Wave Propagation in a Random Medium* (McGraw-Hill, New York, 1960).

17. We thank F. DiNapoli and O. Diachok for the source and vertical receiving array; G. Kudlak, D. Hicks, and R. Dicus for technical assistance; and E. Scheer and J. Polcari for providing programs for the primary data reduction. Supported by the Office of Naval Research, Arctic Programs.

19 May 1986; accepted 20 January 1987

Physical Properties of Sea Ice Discharged from Fram Strait

ANTHONY J. GOW AND WALTER B. TUCKER III

It is estimated that 84 percent of the ice exiting the Arctic Basin through Fram Strait during June and July 1984 was multiyear ice and that a large percentage of this ice is ridged or otherwise deformed. While freeboard and thickness data, together with salinity measurements on cores, usually sufficed to distinguish between first and multiyear floes, preliminary identification could usually be made on the basis of snow cover measurements with snow cover being much thicker on multiyear ice. Cores from the top half meter of multiyear floes were generally very much harder and more transparent than cores from first-year floes. Age estimates of multiyear floes, based on petrographic and salinity characteristics of cores, did not exceed 4 to 5 years for any of the floes that were observed exiting Fram Strait.

DURING JUNE AND JULY 1984, INVESTIGATIONS of the physical properties of sea ice were conducted from the German icebreaker *Polarstern* as part of the Marginal Ice Zone Experiment (MIZEX-84). A large area within the Fram Strait was traversed by *Polarstern* and provided an opportunity to obtain core samples from 40 separate floes that had likely originated in different parts of the Arctic Basin. Fram Strait is located between the East Greenland coast and Spitsbergen and is the

U.S. Army Cold Regions Research and Engineering Laboratory, Hanover, NH 03755.

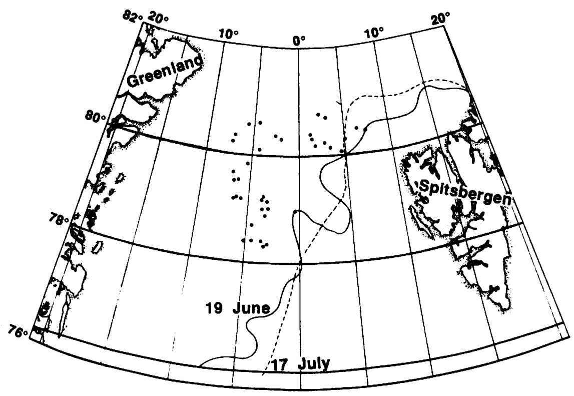

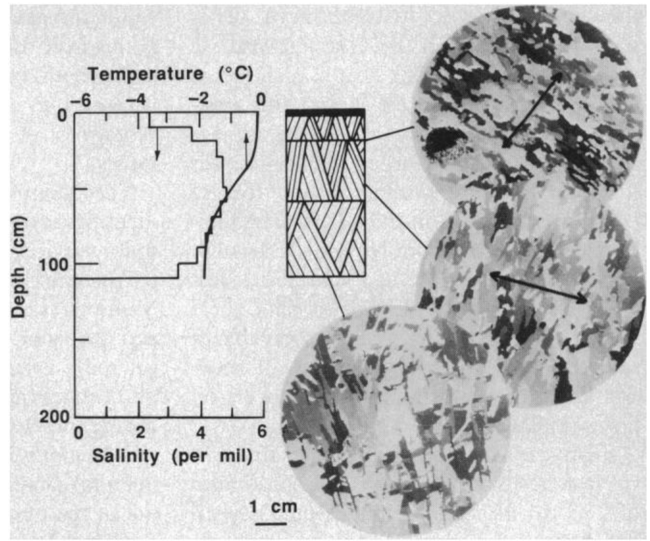

Fig. 1 (**left**). Floe sampling sites (filled circles) in Fram Strait. Approximate positions of the ice edge on 19 June and 17 July 1984 are also indicated. **Fig. 2** (**right**). Salinity, temperature, and structure profiles of a first-year ice floe from Fram Strait. The floe consists of 95% congelation ice. Arrows on the photographs of horizontal thin sections indicate the direction of the current-controlled orientation (preferred *c*-axis) of sea ice crystals.

major outflow region of ice from the Arctic Basin. The volume of ice outflow is highly variable, both seasonally and annually (*1*). However, estimates generally agree on an average transport of about 0.1 Sverdrup (*2*). The discharge volume of ice through other passages from the Arctic Basin (for example, Bering Strait or the Canadian Archipelago) is considered negligible by comparison (*2*).

The locations of sampling sites are shown in Fig. 1. Sampling covered a geographical area that extended from 78°20′N to 80°42′N latitude and from 7°16′E to 7°10′W longitude. Individual floes were reached either directly from the side of *Polarstern* or by helicopter. Forty individual floes with diameters that ranged from 100 m to several kilometers were sampled, occasionally at more than one location on the same floe. Core drilling was performed at 54 separate sites. A total of 243.18 m of core was obtained, all but 5.01 m of which was used for salinity and structural analysis.

Two cores were taken through the entire thickness of ice at each site. The larger of the two cores measured 10 cm in diameter and was returned to the ship for structural analysis. The second core, which measured 7.5 cm in diameter, was used for ice temperature and salinity measurements. Salinity samples were prepared from 10-cm-long core segments that were placed in sealed containers and then returned to the ship where they were melted for salinity analysis (*3*).

A 0.5-cm-thick vertical slice of ice was cut from along the entire length of each structure core 10 cm in diameter and examined between crossed polaroids to evaluate the crystalline texture and structure of ice in the floe. Horizontal thin-section samples were then selected at intervals along the core and sliced to a thickness of 0.2 to 0.5 mm on a microtome to examine the crystalline structure in greater detail.

A schematic depiction of crystalline texture, in vertical section, together with selected horizontal thin-section structure photographs and temperature and salinity profiles, were then prepared for cores from each floe. Representative examples from a first and multiyear ice floe are shown in Figs. 2 and 3, respectively.

Structurally, 75% of the ice we examined consisted of columnar, vertically elongated crystals that were formed by direct freezing (congelation) of sea water to the underside of the ice sheet. Granular ice, mainly frazil, thus represented only about 25% of the total ice in the 40 floes we examined, and in undeformed floes frazil averaged less than 15% of the total ice thickness. It was found in small amounts in the surface layers of most floes (often in conjunction with snow ice) and in larger amounts (up to 71%) in old ridges where it occurred mainly as the material that filled the voids between ice blocks. However, the frazil content of Fram Strait floes is very much less than those observed in floes in the Weddell Sea, Antarctica, where it is estimated that it represents 50 to 60% of the total ice in the Weddell Sea ice pack (*4*). Such a contrast indicates that there are significant differences in oceanic structure and circulation between the Arctic Basin and the Weddell Sea.

A standard taxonomy exists for the classification of sea ice based on its stage of growth (*5*). The definition of multiyear ice according to (*5*) requires that it have survived two summers. However, the distinction between multiyear ice and second-year ice is subtle and here we make only the larger distinction between first-year ice and other ice that has survived at least one summer, or multiyear ice.

Of the 40 individual floes sampled, 27 were identified as multiyear, 9 were first year, and 4 were composite floes made up of a combination of first-year and multiyear ice. These composite floes usually consisted of undeformed first-year ice attached to multiyear floes. Because we sampled first-year ice whenever the opportunity arose, the percentage of first-year ice we examined was biased toward higher values than actually existed in the region. However, on the basis of the number fraction of multiyear to first-year ice floes examined, we estimate that the fraction of multiyear ice would exceed 75% in most areas transited by the *Polarstern*. On a volume basis, if we assume that multiyear floes are on average 70% thicker than first-year floes, multiyear ice would constitute more than 84% of the volume of ice discharged from Fram Strait during this period. This contrasts significantly with earlier estimates, such as those based on visual observations on bird's-eye flights (*6*) which indicated that multiyear ice represented less than 40% of the spring-summer transition (June and July) ice cover in the Greenland Sea. There are two possibilities for the low percentage of first-year ice. The first is that first-year ice does not exist in large quantities in the source regions that were responsible for generating the ice that transited Fram Strait during MIZEX-84. The second possibility is that much of the first-year ice is deformed and crushed before it enters the Fram Strait.

Snow depths on multiyear ice ranged from 3 to 65 cm and averaged 29 cm. On first-year ice the snow cover was much thinner and averaged only 8 cm; it never exceeded 20 cm. This difference in the amount of accumulated snow proved such a reliable criterion of ice type that provisional identification of first and multiyear floes could generally be made on this basis. Preliminary calculations based on snow ablation modeling showed that it is possible for the thinner first-year ice to lose much of its snow by sublimation. Because first-year ice is relatively thin, more heat is conducted from the ocean to the ice surface and sensible and latent heat losses to the atmosphere are correspondingly larger than those for thick ice. Modeling results for snow-free ice (*7*) showed that 3.0-m-thick ice had negligible latent-heat loss from November through May while thinner ice had substantial heat loss. Thus the transfer of oceanic heat through young sea ice is believed capable of sublimating substantial quantities of snow and leads to much thinner snow covers on first-year floes.

First-year ice thicknesses ranged from 38 cm in a newly refrozen lead to a maximum of 236 cm in a floe that measured several kilometers in diameter. Multiyear ice thicknesses ranged from 174 cm to 536 cm with the thicker of these coming from old ridge fragments. The greatest thickness observed that showed no evidence of previous deformation was 411 cm, but of seven floes that exceeded 3.5 m in thickness, six were of previously deformed ice. Ten of the 31 multiyear cores retrieved were identified as having been drilled in ridged ice. Although we never purposely drilled into ridged ice, the fact that one-third of our multiyear ice cores contained ridged ice indicated that multiyear floes may have been composed of significant amounts of deformed ice that had no intrinsic surface expression. Indeed, multiyear floes may survive for several years because they are composed of a large percentage of stronger and thicker multiyear ridges.

The salinity profiles usually permitted identification of the ice as either first-year or multiyear ice, especially in cases where the ice thickness may have indicated otherwise. Multiyear ice salinity averaged 2.1 per mil, and the salinity was generally very low (<1 per mil) in the upper layers of floes because of flushing and extensive brine drainage during previous summers. We found the mean salinity of first-year ice to be 4.0 per mil with salinities usually greater than 2 per mil in the upper layers. As the melt period progressed from mid-June to mid-July the mean salinity of the first-year ice decreased about 1 per mil while that of the multiyear ice increased by about 0.3 per mil. Figure 4 shows the variation of mean salinity with ice thickness for both ice types. Both show a slight salinity increase with ice thickness. The least-squares fit for multiyear data is in excellent agreement with that found for warm, predominantly Beaufort Sea ice (*8*).

Identification of multiyear ice on the basis of freeboards or drilled thickness or both was not always reliable, especially in the region of thickness overlap where the thinnest multiyear ice (1.7 to 1.8 m) was appreciably thinner than the thickest first-year ice (2.3 m thick). However, even if snow layer thickness considerations are ignored, positive identification of multiyear ice could usually be made from observations of the appearance and mechanical condition of ice cores in the top meter of a floe. First-year ice is characteristically opaque, mainly because of the light-scattering effect of the numerous brine pockets located within the substructure of the sea ice crystals. However, our experience in Fram Strait was that the top 0.5 to 1.0 m of ice in multiyear floes is (i)

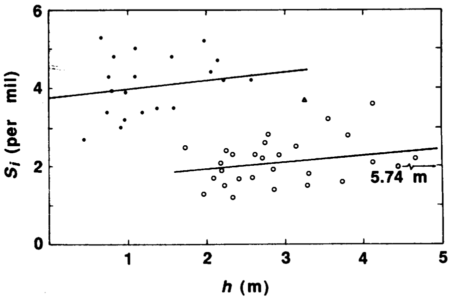

Fig. 4. Plots of bulk salinity versus thickness of first-year and multiyear ice floes in Fram Strait. The best linear regression fit for the upper line is $S_i = 3.75 + 0.22h$, and for the lower line is $S_i = 1.58 + 0.18\,h$, where S_i is salinity and h is ice thickness. Closed circles are first-year ice; open circles are multiyear ice; the triangle is first-year ridge ice.

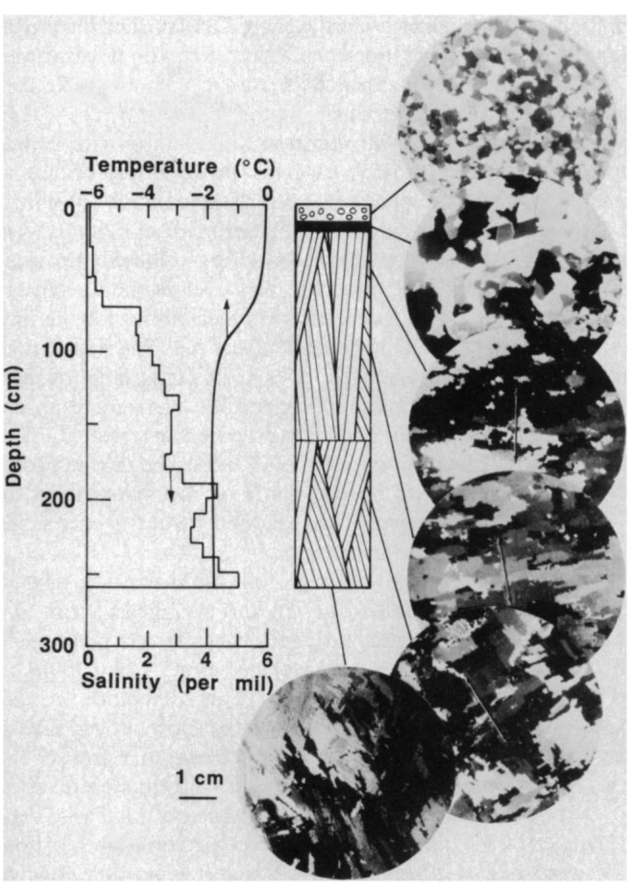

Fig. 3. Salinity, temperature, and structure profiles of a multiyear ice floe composed of 93% congelation ice.

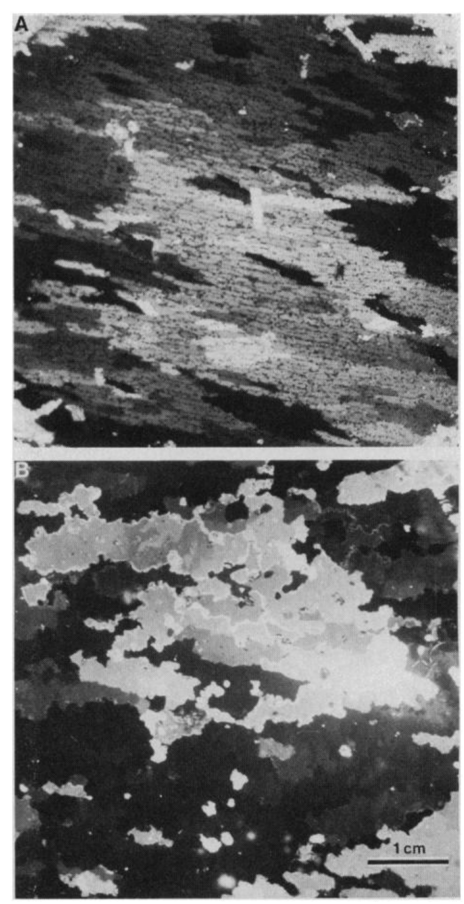

Fig. 5. (**A**) Thin section of first-year sea ice that exhibited oriented ice plate and brine layer substructure compared to that of (**B**) which is retextured, brine-drained ice of multiyear floe. Note that despite retexturing the original alignment of crystals was retained.

much less opaque and often semitransparent in appearance, and (ii) much more resistant to drilling and sawing than first-year ice. These changes are attributed to the exposure of the ice to elevated temperature and solar radiation during the previous summer or summers, which not only results in substantial loss of brine, as borne out by salinity measurements, but also produces significant changes in the crystalline texture of the ice. These changes include major modification of the ice plate and brine lamella substructure of crystals, sometimes to the point of virtually complete obliteration of brine pockets, and substantial smoothing out of the typically angular, interpenetrated outlines of the crystals themselves. We term such textural modification as retexturing. An example of such structure and that of fresh, unmodified congelation ice is shown in Fig. 5, A and B. This retexturing, which was observed to depths of a meter or more, is probably equivalent to the so-called recrystallization inferred from microwave measurements (*9*) to have occurred in the upper levels of multiyear ice in the Beaufort Sea.

Retexturing of sea ice occurs simultaneously with flushing of summer surface melt water, which is the principal mechanism by which brine is drained downward from the floe to create ice with multiyear salinity characteristics. Ultimately the ice at the top of the floe, which is retextured, glacier-like, and brine-poor, bears little resemblance to the original sea ice. Such modification should result in significant changes in the mechanical and electromagnetic properties of this ice and in its response to remote-sensing signals.

Although drilling the top meter or so of floes generally sufficed to distinguish between first-year and multiyear ice types, complete drilling of a multiyear floe is needed to obtain an estimate of its age. Most floes show some evidence of aligned *c*-axis structure related to the growth of ice under the direct influence of currents at the growing ice interface (*10*). Alignment changes in a multiyear floe thus constitute a record of the orientation of the floe with respect to the direction of current motion directly beneath the ice. We assume that the alignment directions of the *c*-axes occur on an annually repeating basis, which is consistent with wintertime growth under conditions of an immobilized or tight pack. Such changes in alignment direction together with crystal size and shape changes and surges in the salinity profile (which often coincide with changes of crystal alignment) can be used to estimate the ages of multiyear floes. Floes demonstrably older than 4 to 5 years were not observed. Conversely, the absence of aligned *c*-axis structure can be correlated most probably with growth during unencumbered drift or rotation of the ice floe with respect to the direction of the current directly beneath the ice. This was a common condition of recently formed or actively growing ice on the bottom of floes as they exited Fram Strait.

REFERENCES AND NOTES

1. T. E. Vinje, *Norsk Polarinstitut Arbok* (1975).
2. V. T. Timofeyev, *Probl. Arktiki Antarkt.* **5**, 27 (1958); K. Aagaard and P. Greisman, *J. Geophys. Res.* **80**, 3821 (1957).
3. Measurements of salinity were made with a temperature-compensating Beckman Solubridge that was periodically calibrated against solutions that were prepared from Copenhagen Standard Seawater (chlorinity of 19.373 per mil). Individual determinations were considered accurate to ±0.2 per mil.
4. A. J. Gow, S. F. Ackley, W. F. Weeks, J. W. Govoni, *Ann. Glaciol.* **3**, 113 (1982); W. F. Weeks and S. F. Ackley, *CRREL Monograph 82-1* (U.S. Army Cold Regions Research and Engineering Laboratory, Hanover, NH, 1982).
5. World Meteorological Organization, *Exec. Comm. Rep.* **8**, 107 (1956).
6. W. I. Wittmann and J. J. Schule, *Proceedings of the Symposium on Arctic Heat Budget, Rep. RM-5233-NSF* (Rand Corporation, Santa Monica, CA, 1966).
7. G. A. Maykut, *J. Geophys. Res.* **83**, 3646 (1978).
8. G. F. N. Cox and W. F. Weeks, *J. Glaciol.* **13**, 109 (1974).
9. D. C. Meeks, G. A. Poe, R. O. Ramseier, *Final Report 1786 FR-1* (Aerojet Electrosystems Co., Azusa, CA, 1974).
10. W. F. Weeks and A. J. Gow, *J. Geophys. Res.* **83**, 5105 (1978); *ibid.* **85**, 1137 (1980).

11. This research was sponsored by the U.S. Office of Naval Research through grant N0001484WRM2406. We thank the MIZEX staff and the scientists and crew aboard *Polarstern* for their cooperation during the MIZEX-84 cruise.

19 May 1986; accepted 16 January 1987

Visualization of Viral Clearance in the Living Animal

ERIC M. VERDIN, ELEFTHERIA MARATOS-FLIER,* C. RONALD KAHN, JEAN-CLAUDE SODOYEZ, FRANCOISE SODOYEZ-GOFFAUX, CLAUDINE J. DE VOS, STEVEN P. LYNN, BERNARD N. FIELDS

The early events in viral dissemination via the bloodstream were identified by monitoring the fate of ^{123}I-radiolabeled reovirus after it was injected intravenously in rats. Continuous scintillation camera imaging showed that reovirus serotypes 1 and 3 were cleared from the circulation in less than 10 minutes by specific and distinct target organs. Reovirus serotype 1 accumulated predominantly in the lungs and the liver, whereas serotype 3 accumulated in the liver and the spleen with very little virus uptake by the lungs. Incubation of reovirus serotype 1 with a monoclonal antibody directed against the viral hemagglutinin before injection totally inhibited the clearance of the virus by the lungs. Similar results were obtained when viruses biolabeled with ^{35}S were used. These results demonstrate that viruses can be rapidly transported through the bloodstream to specific target organs and that the localization of the viruses depends on the interaction between specific viral surface components and the target organ.

AFTER ENTERING A HOST AND MULTIPLYING at the site of entry, viruses may reach the bloodstream, usually by way of the lymphatic system. Once in the circulation, a virus can potentially localize in any organ of the body within seconds. These early events probably determine the capacity of a virus to reach a target organ distant from the site of entry or to initiate a systemic infection within a host (*1*). However, the rapidity with which viruses are cleared from the bloodstream and problems inherent to the quantitative recovery of infectious particles from various organs (*2*) have limited the study of these important early events in a whole animal.

We have used the mammalian reoviruses to analyze how viruses may use the bloodstream to spread within a host. The mammalian reoviruses are small (diameter, 70 nm), icosahedral, nonenveloped viruses containing double-stranded RNA genomes whose natural hosts include humans, rodents, and bovids (*2, 3*). Three serotypes, designated 1, 2, and 3, are recognized by their differing neutralization and hemagglutination patterns (*4*). Genetic studies have enabled the contribution of the individual viral proteins in the pathogenesis of reovirus infection to be defined (*5*). Protein σ1, located in the outer capsid of the virus, is responsible for serotype-specific immunologic properties,

E. M. Verdin, E. Maratos-Flier, C. R. Kahn, Research Division, Joslin Diabetes Center, Boston, MA 02215, and Department of Medicine, Brigham and Women's Hospital, Boston, MA 02215.
J.-C. Sodoyez, F. Sodoyez-Goffaux, C. J. De Vos, Department of Internal Medicine and Pediatrics, Hôpital de Bavière, Université de Liège, Liège, Belgium.
S. P. Lynn, Department of Microbiology and Molecular Genetics, Harvard Medical School, Boston, MA 02115.
B. N. Fields, Department of Microbiology and Molecular Genetics, Harvard Medical School, and Shipley Institute of Medicine and Department of Medicine, Division of Infectious Disease, Brigham and Women's Hospital, Boston, MA 02115.

*To whom correspondence should be addressed.